

Changes in the Modulation Amplitude and the Particle Sizes of Co/Pd Multilayers During Stress Release and Interdiffusion

Jai-Young Kim* and Jan E. Evetts

Department of Materials Science and Metallurgy, Faculty of Physics and Chemistry, University of Cambridge, Pembroke Street, Cambridge CB2 3QZ, United Kingdom

**Analytical Engineering Lab., Corporate Technology Consulting & Services Center, Samsung Advanced Institute of Technology, P.O. Box 111, Suwon, Korea 440-600*

(Received 21 August 1997)

An artificially modulated magnetic Co/Pd multilayer is one of the promising candidates for high density magneto-optic (MO) recording media, due to large Kerr rotation angle in the wavelength of a blue laser beam. However, since multilayer structure, as well as amorphous structure, is a non-equilibrium state in terms of free energy and MO recording is a kind of thermal recording which is conducted around Curie temperature (T_C) of the recording media, when the multilayer is used for the MO recording media, changes in the multilayer structure are occurred as the amorphous structure do. Therefore, the assessment of the structural stability in the Co/Pd multilayer is crucially important both for basic research and applications. As the parameter of the structural stability in this research, modulation amplitude and particle size of the Co/Pd multilayer are measured in terms of Ar sputtering pressure and heat treatment temperature. From the results of the research, we find out that the magnetic exchange energy between Co and Pd sublayers strongly affects the changes both of the modulation amplitude and the particle size of the Co/Pd multilayers, when heat treated below T_C . This discovery will provide the understanding of the magnetic exchange energy in the structural changes of a magnetic multilayer structure and suggest the operating temperature range for MO recording in the Co/Pd multilayer for the basic research and applications, respectively.

1. Introduction

It is well recognized that magneto-optic (MO) recording offers remarkable performance, with a greater recording capacity than a hard disc and a better access time than a floppy disc. Presently, popular MO recording wavelengths and materials are mainly red laser beams (635 - 780 nm) and amorphous HRE-TM (heavy rare earth-transition metal) alloys, respectively. However, from the view of high density MO recording, it is pointed out that corrosion of the rare-earth elements and the reduction of the Kerr effect in a short wavelength of the blue laser beam (~400 nm) cannot be avoided in these amorphous alloys. To solve these problems, a Co/Pd multilayer has been introduced for the next generation of the high density MO recording material [1][2][3][4][5]. Since the Co/Pd multilayer does not contain any rare-earth element, it hardly corrodes. The Co/Pd multilayer also possesses an enhanced Kerr effect in the short wavelength of the blue

laser beam relative to the currently used amorphous alloys. Ultimately, the MO recording and the Co/Pd multilayer seem to be the most promising recording technology and material for high density information storage in the next generation.

The multilayer structure, as well as the amorphous structure, is a non-equilibrium state in terms of free energy[6][7]. Furthermore, MO recording is a kind of thermal recording which is conducted around Curie temperature(T_C)[8] of a recording material. In the non-equilibrium state and the thermal recording, if the Co/Pd multilayer is used for the MO recording material, changes in the multilayer structure are introduced by stress release and interdiffusion with the repeated radiation of a laser beam, and these affect the magnetic and MO properties[9][10] as do the structure relaxation and the crystallization in the amorphous alloys. However, despite the superiority of the Co/Pd multilayer as MO recording material, research into structural stability during the stress

release and the interdiffusion has hardly conducted on it.

In this research, the structural properties of the Co/Pd multilayers during the stress release and the interdiffusion will be discussed in terms of Ar sputtering pressure and heat treatment temperature as parameters of multilayer characteristic and MO recording, respectively. Since the multilayer deposited at lower sputtering pressure, gives a more stable multilayer structure [11][12][13] than at higher sputtering pressure which possesses excellent magnetic properties [11][14], the properties of the multilayers deposited at different sputtering pressures have been analyzed and discussed. In the range of the heat-treatment temperature, when considering MO recording applications, TC is one of the important parameters. So the heat treatment for the stress release and the interdiffusion is conducted in two groups; one below TC and the other above TC. The interdiffusion process of the Co/Pd multilayers was presented elsewhere [15].

2. Experimental Procedure

The Co/Pd multilayers were deposited on R-plane sapphire substrate ($2\theta = 25.60^\circ$ and 52.50°) in a two-target UHV (Ultra High Vacuum) dc magnetron sputtering system which was gettered with liquid nitrogen. The configuration of the sputtering system is described elsewhere [16][17]. The substrates sat on a rotating holder and passed alternately beneath the two magnetrons on which the targets of Co and Pd were attached. A fixed shield was positioned between the level of the magnetrons and that of the substrate holder, with slots cut beneath the magnetrons. The target-substrate distances were 30 mm and 40 mm for the Co and Pd, respectively. The vacuum system was pumped down to 10^{-10} Torr by a liquid nitrogen trapped diffusion pump. The sputtering gas was Ar (99.999%), processed with an Ar purifier. The sputtering pressures were at 0.7 Pa (Sample No. 4457) and 2.0 Pa (Sample No. 4461) in the low and the high pressure runs, respectively. The multilayers had 200 periods and total effective layer thicknesses were designed about 4000\AA for both of the multilayers deposited at 0.7 Pa and 2.0 Pa. The Co sublayer thickness was designed to obtain perpendicular magnetic anisotropy (less than 8\AA) (14) and maximum magnetostriction (30 at. % of Co) (5).

The compositions of the multilayers were determined using an EDS (Energy Disperse Spectrometer). Curie temperature of the Co/Pd multilayers (T_c) was determined by DSC (Differential Scanning Calorimeter) with a heating rate of $40^\circ\text{C}/\text{min}$ and was $368 \pm 5^\circ\text{C}$. The multilayer structure of the as-deposited and heat-treated Co/Pd multilayers were measured by a XRD (X-Ray Diffractometer), using small angle ($2\theta = 3^\circ - 10^\circ$) and medium one ($2\theta = 35^\circ - 50^\circ$) X-ray diffraction with $\theta - 2\theta$ scanning Cu $K\alpha$ ($\lambda = 1.5406\text{\AA}$) radiation was used in the

XRD. In order to measure the X-ray intensities precisely, scans of rocking curve and calibration of 2θ -off method were adapted. The wavelengths of the Co/Pd multilayers were deduced from the positions of satellite peaks in the small angle region. The nominal sublayer thickness of each element was calculated by combining the atomic weight ratio of the composition in the multilayer, assuming that the bulk densities of pure metals could be applied. \pm

The multilayers to be heat-treated were inserted in quartz ampoules. The ampoules were sealed after being pumped up to 10^{-6} Torr and filled again with pure argon to about 200 Torr to insure good thermal contact between the sample and surroundings during heat treatment. The temperature of heat treatment for the structural changes was divided into two groups under the consideration of application in MO recording. One was below T_c , 250°C and 350°C and the other was above T_c , 390°C and 400°C .

3. Results and Discussion

According to the composition analyses by EDS, average compositions of the multilayers deposited at 0.7 Pa and 2.0 Pa are 29.9 ± 0.2 at. % Co and 29.2 ± 0.4 at. % Co respectively. Since the difference in composition between the multilayers is less than 3 % of each other, it will not seriously affect the main experiment which will compare the multilayers deposited with the same composition but different sputtering pressure. In the structural change of the Co/Pd multilayer during the stress release and the interdiffusion, the modulation amplitude in harmonic wavelength and the particle size in multilayer matrix will be evaluated as chemical order and structural order, respectively.

3. 1. Change of the modulation amplitude in Co/Pd multilayers during stress release and interdiffusion

Fig. 1 (a) and (b) display one of the X-ray diffraction satellite peaks in the small angle region ($2\theta = 3^\circ - 10^\circ$) for Co/Pd multilayers deposited at 0.7 Pa and 2.0 Pa, respectively. The first and the second satellite peaks are detected in these multilayer structures. The average position of the first satellite peaks are $2\theta = 4.81^\circ \pm 0.14^\circ$ and $4.73^\circ \pm 0.09^\circ$, and which are corresponding to the modulation wavelength of $\lambda = 18.36\text{\AA}$ (Co = 4.44\AA , Pd = 13.92\AA) and 18.69\AA (Co = 4.39\AA , Pd = 14.30\AA) for the multilayers deposited at 0.7 Pa and 2.0 Pa, respectively. The difference in the average wavelength of the multilayers may have been caused by the difference in the average composition of the multilayers and the contribution of micro voids created in the higher sputtering pressure [11][14][18].

Since the X-ray intensity of the multilayer deposited at 0.7 Pa is larger than that at 2.0 Pa and the intensity is

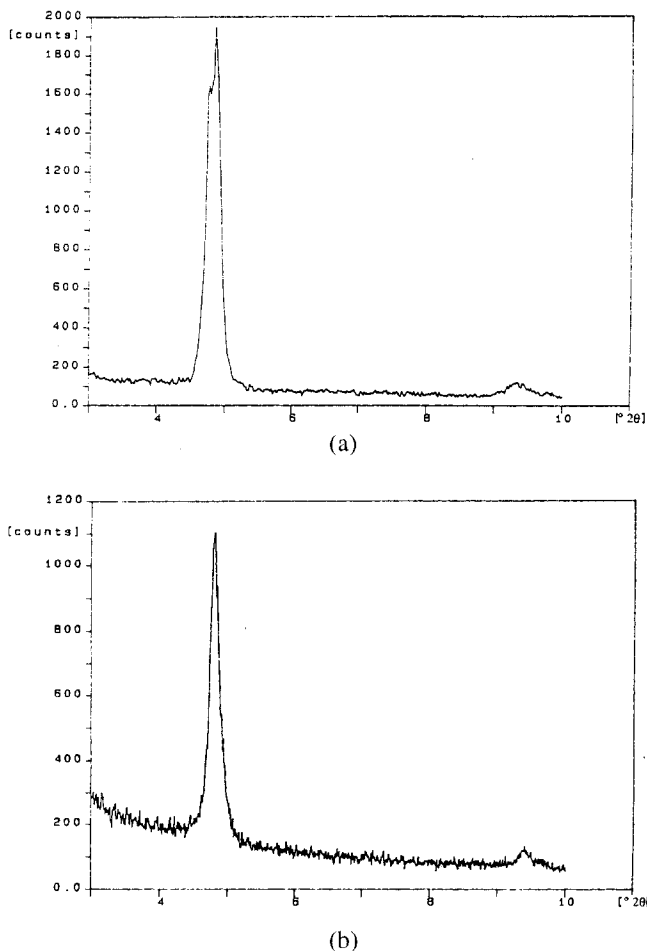


Fig.1. (a) and (b): X-ray diffraction satellite peaks in the small angle region ($2\theta = 3^\circ - 10^\circ$) for Co/Pd multilayers deposited at 0.7 and 2.0 Pa, respectively

proportional to square of modulation amplitude[19], the interfaces of the multilayer deposited at 0.7 Pa appear sharper than that at 2.0 Pa. The interfacial roughness in multilayer structure as the parameter of an interfacial sharpness can be estimated from the following equation[20][21][22]

$$I \propto \frac{1}{\sin^4\theta} \exp\left\{-2\left(\frac{2\pi\sigma\sin\theta}{\lambda_x}\right)^2\right\} \quad (1)$$

- I: First satellite peak intensity of multilayer
- σ : Roughness at the interface of multilayer
- θ : Bragg angle corresponding to composition modulation
- λ_x : X-ray wavelength

A plot of $\ln(I\sin^4\theta)$ versus $\sin^2\theta$ should thus approximate a straight line whose gradient becomes steeper as σ grows larger. The estimated average roughness at the interface deposited at 0.7 Pa is $3.85 \pm 0.04\text{\AA}$ and that at 2.0 Pa is $4.27 \pm 0.15\text{\AA}$, which is coincident with the result of the X-ray diffraction curves in the Co/Pd multilayers of Fig. 1 (a) and (b).

Fig. 2 shows one of the X-ray diffraction curves of as-

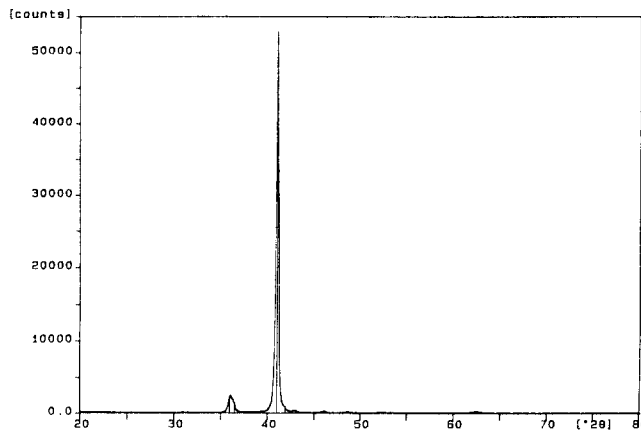


Fig.2. X-ray diffraction curve in the medium angle range ($2\theta = 20^\circ - 80^\circ$) for as-deposited Co/Pd multilayer

deposited Co/Pd multilayers measured in the medium angle range ($2\theta = 20^\circ - 80^\circ$). Fig. 3 is the magnification of Fig. 2 in X-ray intensity. On the figures, the main Bragg diffraction peak corresponding to Co/Pd multilayer structure is $2\theta = 41.00^\circ$, and the lower and higher satellite peaks due to the composition modulated structure are $2\theta = 36.46^\circ$ and 46.17° , respectively. The rest of the peaks are caused by the R-plane sapphire substrate ($2\theta = 25.60^\circ$ and 52.50°) and the XRD sample holder. The Bragg peak for bulk Co in [111] of the cubic structure is $2\theta = 44.22^\circ$ [23] or that in [0001] of hexagonal structure[24] is $2\theta = 44.76^\circ$, and the one for Pd in [111] of cubic structure is $2\theta = 40.11^\circ$ [25]. Instead of the peak positions for pure Co and Pd elements, single large diffraction peak which corresponds to the Co/Pd multilayer structure is measured between those of the pure Co and Pd elements in the diffraction curve. However, the single diffracted peak is not positioned at an approximate average between those of the pure Co and Pd elements. The diffracted peak position of the Co/Pd multilayer structure shown in Fig. 2 is rather close to that of pure [111] Pd element than those of pure fcc [111] or hep [0001] Co. This means that lattice parameter of the Co/Pd multilayer is extended compared with that of the Co/Pd multilayer in perfectly coherent state. The coherent strain at the interface of the Co/Pd multilayer which is deposited by sputtering method is released by misfit dislocations and partial coherent state is maintained at the interface of the Co/Pd multilayer. In previous research[26], it was stated that Co/Pd multilayers deposited by a sputtering process displayed a preferential $\langle 111 \rangle$ textured matrix growing perpendicular to the multilayer plane. The growth of a textured matrix in sputtered Co/Pd multilayers can be regarded as follows; at the initial stage, epitaxial growth takes place, and coherent interfaces are maintained in the perpendicular direction to the substrate. However, this condition cannot last until the end of growth. Some impurities, for example energetic

bombardment of neutralized Ar gas, are involved at the interface and break the coherent state in the multilayer[27]. Therefore, the Co/Pd multilayers deposited in the UHV dc magnetron sputtering system are regarded as a textured polycrystalline structure normal to the substrate.

In previous research[28][29], the existence of a large coherent strain for epitaxial growth in <100> textured Co/Pd multilayers was detected at the interface, but no appreciable coherent strain arising from the <111> textured multilayer was found. Since the Co/Pd multilayers examined in this experiment are <111> textured polycrystalline multilayers, only the modulation amplitude for Co/Pd multilayers in incoherent state is calculated. The equation for the modulation amplitude (A) is presented as follows[30],

$$\frac{I_{+1}}{I_B} = \frac{A^2}{4} \left[\frac{f_d}{F} + \lambda \epsilon \left(\frac{1}{d} - \frac{1}{\lambda} \right) \right]^2 \quad (2)$$

and

$$\frac{I_{-1}}{I_B} = \frac{A^2}{4} \left[\frac{f_d}{F} + \lambda \epsilon \left(\frac{1}{d} - \frac{1}{\lambda} \right) \right]^2 \quad (3)$$

I_{-1}, I_{+1} : Intensity of the first lower and higher satellite peak, respectively

I_B : Intensity of the Bragg peak

where

$$F = C_{Co}f_{Co} + (1 - C_{Co})f_{Pd}$$

$$f_d = f_{Co} - f_{Pd}$$

$$\epsilon = (d_{Co} - d_{Pd})/d$$

C_{Co} : Molar fraction of Co

f_{Co}, f_{Pd} : Atomic scattering factors of Co and Pd at the scattering vector s ($= 2 \sin\theta/\lambda$)

ϵ : Lattice strain in incoherent interface

d_{Co}, d_{Pd} : Lattice spacing of Co and Pd, respectively

d : Average lattice spacing of Co/Pd multilayer

λ : Modulation wavelength

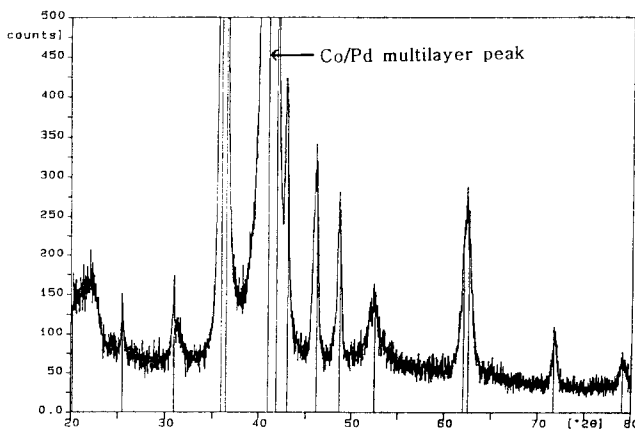


Fig.3 Magnification of Fig. 2 in X-ray intensity

Table 1: Incoherent strains and modulation amplitude of the Co/Pd multilayers deposited at 0.7 Pa and 2.0 Pa

Multilayer	Strain (%)	I_{-1}/I_B	I_{+1}/I_B	Amplitude (I_{-1}/I_B) (%)	Amplitude (I_{+1}/I_B) (%)
0.7 Pa (for 250°C)	9.09	0.1539	0.0015	66.04	51.84
0.7 Pa (for 350°C)	9.07	0.0446	0.0023	35.66	66.92
0.7 Pa (for 390°C)	9.10	0.2519	0.0020	85.57	66.86
0.7 Pa (for 400°C)	9.07	0.1259	0.0046	58.56	78.89
2.0 Pa (for 250°C)	9.08	0.0597	0.0034	41.22	78.16
2.0 Pa (for 350°C)	9.09	0.0789	0.0018	35.39	53.73
2.0 Pa (for 390°C)	9.06	0.0528	0.0054	37.93	85.01
2.0 Pa (for 400°C)	9.06	0.0503	0.0022	37.18	55.24

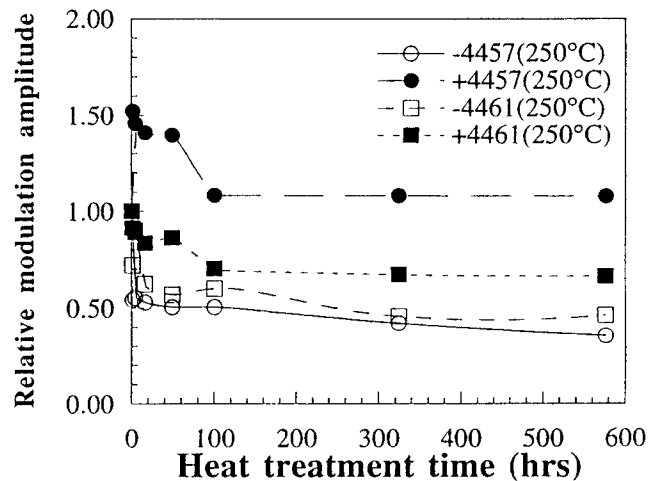


Fig.4: Relative modulation amplitude of Co/Pd multilayers deposited at 0.7 Pa and 2.0 Pa, and heat treated at 250°C as a function of heat treatment time

Table 1 displays the incoherent strains[31] and their modulation amplitude of the as-deposited Co/Pd multilayers, where I_{-1} and I_{+1} represent the intensities of lower and higher satellite peak around diffracted multilayer structure peak, respectively. I_B stands for the intensity of the diffracted multilayer structure peak. The modulation amplitudes caused by the lower (I_{-1}/I_B) and higher (I_{+1}/I_B) satellite peak are not equal to each other. This means that the interface is not in a perfect but a partial coherent state,

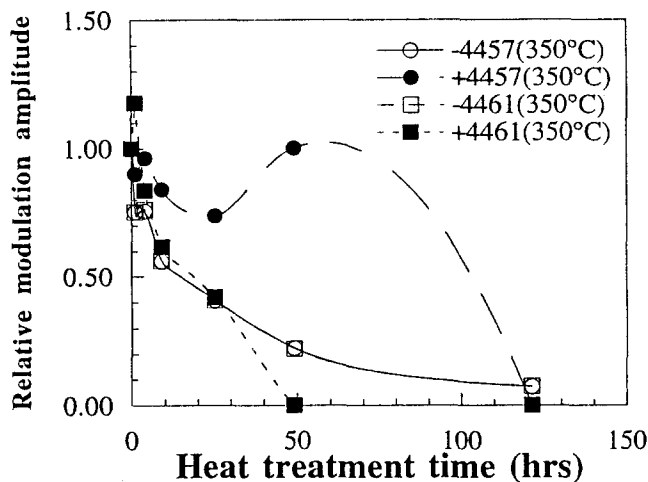


Fig.5: Relative modulation amplitude of Co/Pd multilayers deposited at 0.7 Pa and 2.0 Pa and 2.0 Pa, and heat treated at 350°C as a function of heat treatment time

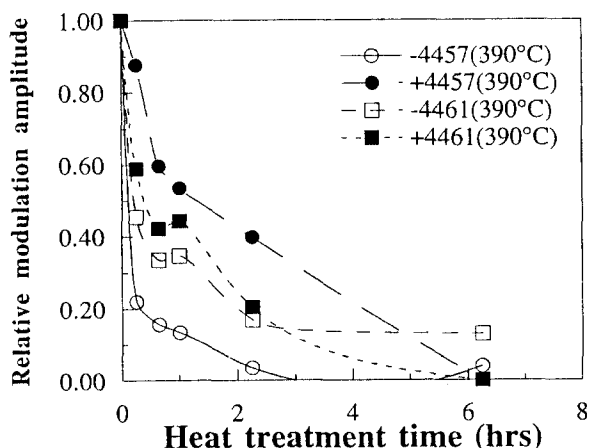


Fig. 6: Relative modulation amplitude of Co/Pd multilayers deposited at 0.7 Pa and 2.0 Pa, and heat treated at 390°C as a function of heat treatment time

which is coincident with the result of the X-ray diffraction curve in the Co/Pd multilayer in Fig. 2 and Fig. 3.

Fig. 4, Fig. 5, Fig. 6 and Fig. 7 represent the changes in relative modulation amplitude of lower and higher satellite peaks around Co/Pd multilayer structure deposited at 0.7 Pa and 2.0 Pa, and heat treated 250°C, 350°C, 390°C and 400°C, respectively. The relative modulation amplitude plots with respect to heat treatment time on Fig. 4 and Fig. 5 are heat treated below T_c , and those on Fig. 6 and Fig. 7 are done above T_c . In the figures, the units on the Y axis are an arbitrary ratio. The arbitrary ratio of 1 represents the modulation amplitude in as-deposited and the unit of 0 stands for the absence of the composition modulated multilayer structure. This means that the first satellite peak in the small angle, which is caused by composition modulation cannot be detected beyond the heat treatment

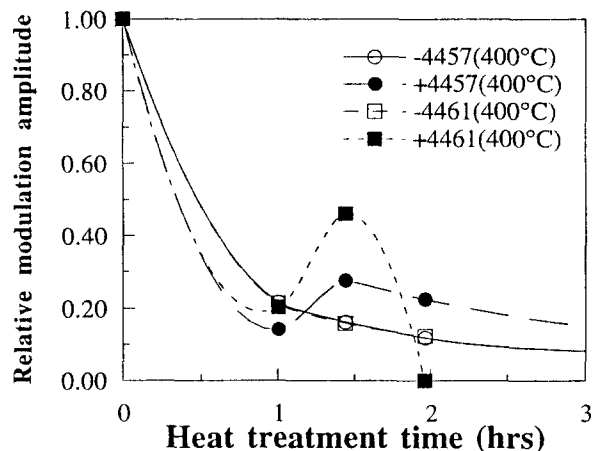


Fig. 7: Relative modulation amplitude of Co/Pd multilayers deposited at 0.7 Pa and 2.0 Pa, and heat treated at 400°C as a function of heat treatment time

time corresponding to 0.

The multilayers deposited at 0.7 Pa and heat-treated at 250°C and 350°C, or deposited at 2.0 Pa and heat-treated at 350°C demonstrate a modulation amplitude of more than 1, which heat-treated below the T_c as shown on Fig. 4 and Fig. 5. The first possibility in increase of the modulation amplitude is due to spinodal decomposition. But because Co-Pd alloy system(32) does not show spinodal decomposition, this possibility is not considered. The second possibility is as follows; As mentioned previously in Fig. 1, the Co/Pd multilayers by sputtering deposition display roughness at the interface, for there is not enough surface mobility at the interface during the deposition. However, the initial stage of heat treatment provides the Co/Pd interface thermal energy in order to conduct surface mobility, so that this leads to an increase in regularity at the interface in the multilayers and an enhancement of the modulation amplitude in the harmonic wave. This is referred to the stress release at the interface of the Co/Pd multilayers. On the other hand, the Co/Pd multilayers heat-treated above the T_c cannot detect the relative modulation amplitude above 1. The interdiffusion process when heat-treated above T_c is so fast that the stress release cannot be measurable. In this heat treatment temperature region, the modulation amplitudes are simply reduced by the alloying at the interface due to the interdiffusion process in the multilayer and finally arrive at 0 of the modulation amplitude.

Generally, the modulation amplitude of the multilayers deposited at 0.7 Pa and heat-treated below T_c collapse more slowly than those deposited at 2.0 Pa and heat-treated above T_c . Little difference in the collapse of the modulation amplitude between the multilayers deposited at 0.7 Pa and 2.0 Pa are shown in the heat treatment temperatures both below and above T_c with respect to the heat treatment time. However, when both of the

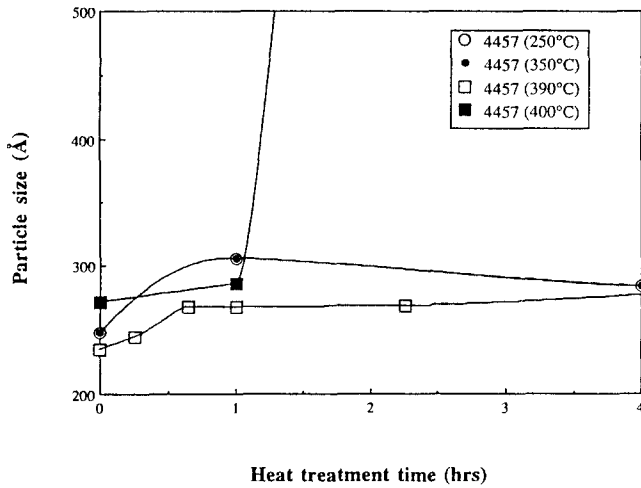


Fig. 8: Particle sizes of Co/Pd multilayers deposited at 0.7 Pa in stress relative region as a function of heat treatment temperature and time

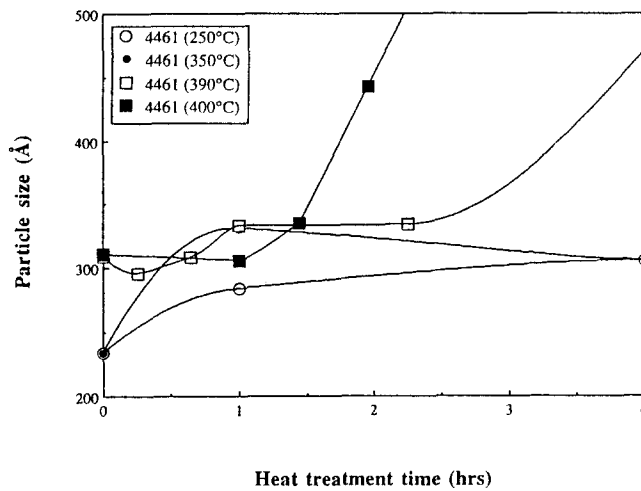


Fig. 9: Particle sizes of Co/Pd multilayers deposited at 2.0 Pa in stress release region as a function of heat treatment temperature and time

multilayers deposited at 0.7 Pa and 2.0 Pa are heat-treated above T_c , their modulation amplitudes collapse very rapidly compared with those heat-treated below T_c , in spite of the small temperature gap. For example, the multilayers heat-treated below T_c (350 °C) and above T_c (390 °C) have their modulation amplitude collapsed around 120 and 3 hours, respectively. This drastic collapse in the chemical order (modulation amplitude) is presumably related to the fast interdiffusion process in the Co/Pd multilayer structure when heat treated above T_c . This will be discussed in Section 3.3 in terms of the effect of magnetic exchange energy on interdiffusion process in the Co/Pd multilayers.

3. 2. Change of the particle size in Co/Pd multilayers during stress release and interdiffusion

Fig. 8 and Fig. 9 show the changes of particle sizes in the Co/Pd multilayers deposited at 0.7 Pa and 2.0 Pa, respectively with respect to initial heat treatment time range. The particle sizes were calculated with the Scherrer formula[33] for the Co/Pd multilayers. The time range on these figures corresponds to the stress release, defined by the modulation amplitude in Fig. 4 and Fig. 5 which are heat treated below T_c . The as-deposited particle sizes of the multilayers at 0.7 Pa and 2.0 Pa were $250 \pm 20 \text{ \AA}$ and $270 \pm 40 \text{ \AA}$, respectively. These are typical particle sizes in thin films and multilayers fabricated by sputtering methods[34][35]. However, because the particle size measurement in the as-deposited state by means of X-ray includes a non-uniform strain effect, the above values can be regarded as only the apparent particle sizes in the non-uniform strain state. The real particle sizes in the Co/Pd multilayers can be obtained only after releasing residual stress by heat treatment. In both figures, it can be seen that the particle sizes approach a fixed particle value which at 0.7 Pa is 283 \AA and at 2.0 Pa is 307 \AA . These values are real particle sizes in the Co/Pd multilayers after releasing the residual stress. The particle sizes of the Co/Pd multilayers heat treated above T_c show rapid divergence from the real particle size in this time range.

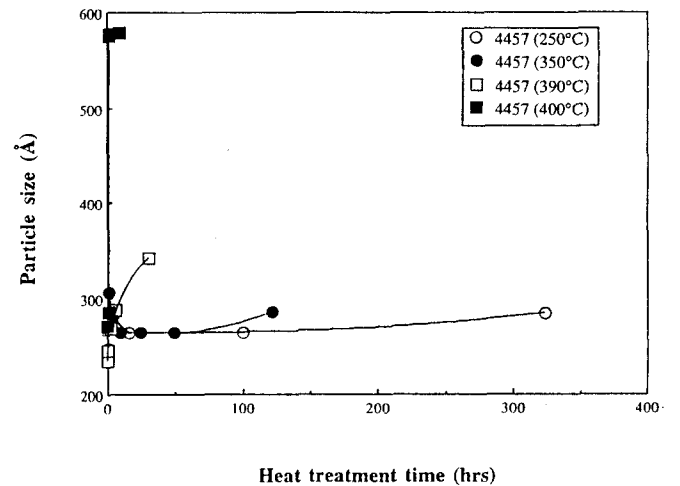


Fig. 10: Particle sizes of Co/Pd multilayers deposited at 0.7 Pa as a function of heat treatment temperature and time

Fig. 10 and Fig. 11 show the changes of the particle sizes in the Co/Pd multilayers deposited at 0.7 Pa and 2.0 Pa, respectively with full heat treatment time range. These figures are divided into 3 parts, the stress release stage mentioned in Fig. 8 and Fig. 9, the interdiffusion stage described in Fig. 4, Fig. 5, Fig. 6 and Fig. 7, and the particle growth developed after the interdiffusion. After the stress release in the Co/Pd multilayers, little change in the particle size is observed in the interdiffusion process on

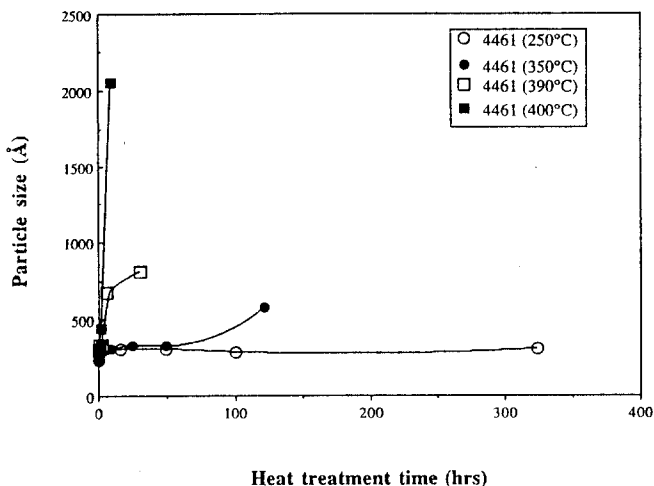


Fig. 11: Particle sizes of Co/Pd multilayers deposited at 2.0 Pa as a function of heat treatment temperature and time

both of the figures, the thermal energy provided by the heat treatment contributes to the interdiffusion process only. As long as the multilayer structure is maintained in Co/Pd multilayers, the particle sizes contained in the multilayers are constant at around 300 Å, even though changes in the modulation amplitudes in the Co/Pd multilayers could be observed in Fig. 4, Fig. 5, Fig. 6 and Fig. 7. So the homogeneous matrix of the multilayers can be maintained until the termination of the interdiffusion.

Comparing these above figures to the figures for the modulation amplitude, it is recognized that the divergence of the particle sizes from around 300 Å appears after the perfect collapse of the modulation amplitude. It means that the thermal energy provided by heat treatment is firstly used for the stress release and the interdiffusion process, then it is used for the growth of particles in the multilayers. The particle sizes of the multilayers deposited at 0.7 Pa and 2.0 Pa grew up to 570 Å and 2000 Å, respectively. The crystal quality of the multilayers resulted from Ar sputtering pressure can affect the growth of particle size. However, on both of the figures, the divergence of the particle size from around 300 Å is not dependent on the sputtering pressure, but mainly on the heat-treated temperature. Both of the multilayers heat-treated above T_c (390°C) diverse within 3 hours, on the other hand those heat-treated below T_c (350°C) diverse around 120 hours, similar to those of the modulation amplitude.

3.3 Effect of magnetic exchange energy on the modulation amplitude and the particle size of Co/Pd multilayers during interdiffusion process

In bulk materials, deviations of diffusion coefficients from Arrhenius behavior in the magnetic phase transition between ferromagnetic and paramagnetic were observed in

the self-diffusion of α -Fe[36][37][38] and the interdiffusion of Co in α -Fe[39]. In these researches, the diffusion coefficients in ferromagnetic region were lower than those in the paramagnetic one. In bulk materials, where all three dimensions are significant, the magnetic bonding force is generally negligible, compared with chemical bonding forces. However, in the multilayer structure, in which only two dimensions need to be considered, the chemical bonding force is weakened due to the loss of symmetry in the crystalline structure, but the magnetic bonding force is significantly enhanced due to the increment of the interfaces per unit volume. Even though the effect of the magnetic exchange energy (E_x) on the diffusion process occurs in both of the multilayer structure and bulk materials, the effect in the former is more predominant than in the latter, due to the increased interfaces per unit volume. When the magnetic multilayer is heat treated below T_c , this enhanced magnetic exchange energy at the interfaces can predominantly contribute to the total bonding force in the multilayer, and a low interdiffusion coefficient is obtained. In the absence of E_x above T_c , only the weakened chemical bonding force exists at the interface and the interdiffusion coefficient is large in the multilayer.

In the case of the Co/Pd multilayers, the unique interdiffusion processes for those heat treated below and above T_c are related to the particular magnetism of Co/Pd multilayers. It is well recognized that the Co/Pd multilayer has a larger saturation magnetization(1)(2) than pure cobalt (1422 emu/cm³)(3)(4)(5), due to induced magnetization in the polarized Pd sublayer. Considering this magnetic phenomenon, the slow interdiffusion process below T_c can be established as follows; when the interdiffusion process is carried out in the Co/Pd multilayer below T_c , the enhanced ferro-magnetic exchange energy exists at the interface between the magnetic Co sublayer and induced magnetic Pd sublayer. This energy can prevent from the interdiffusion at the interface by increasing the total bonding energy, so the interdiffusion process is slow. On the other hand, in the case of the interdiffusion above T_c , there is no E_x at the interface as a barrier against the interdiffusion process. This can promote the interdiffusion process at the interface between non magnetic Co sublayer and non magnetic Pd sublayer, so the interdiffusion process is fast.

Estimated E_x between the magnetic Co sublayer and the polarized magnetic Pd sublayer at the interface is calculated under the following assumptions. One is that magnetic exchange forces decrease rapidly with distance, so that E_x is effective only between the 1st nearest neighbor pairs. The other is that the polarization of Pd occurs in all Pd sublayers, not in those near to the interfaces of the multilayer. Then, E_x is described as below[40],

$$E_x = Z(-2 J_{ex} J_{Co} J_{Pd} \cos\theta) \quad (4)$$

Z: Co-ordination number in Co/Pd multilayer (=12)

J_{ex} : Exchange integral (Joule/mole)

J_{Co} , J_{Pd} : Total angular momentum of Co and Pd, respectively

θ : Angle between two spin moments

$$J_{ex} = \frac{3kT_C}{2ZJ(J+1)} \quad (5)$$

k: Boltzman constant (1.38×10^{-23} Joule/K)

T_C : Curie temperature (641 K in the Co/Pd multilayer)

E_x of the Co/Pd multilayers are as follows,

1) $J = J_{Co} = J_{Pd} = 1/2$ (all pure spin angular momentum)

$$J_{ex} = 0.167kT_C = 1.475 \times 10^{-21} \text{ Joule/atom}$$

$$E_x = -8.851 \times 10^{-21} \text{ Joule/atom}$$

2) $J_{Co} = 1/2$, $J_{Pd} = 1$ (additional orbital momentum due to induced magnetization)

a) $J_{ex} = 0.125kT_C = 1.106 \times 10^{-21}$ Joule/atom

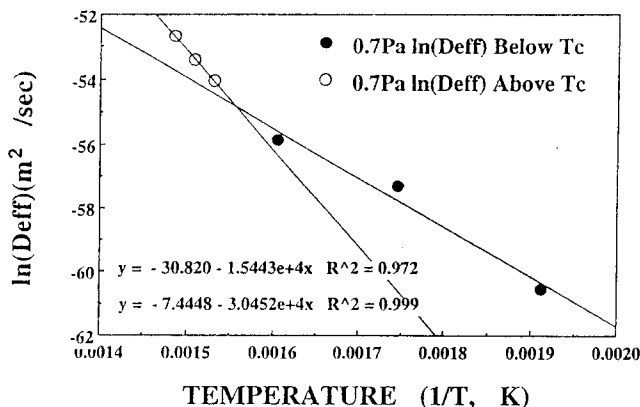
$$E_x = -13.274 \times 10^{-21} \text{ Joule/atom}$$

b) $J_{ex} = 0.083kT_C = 0.737 \times 10^{-21}$ Joule/atom

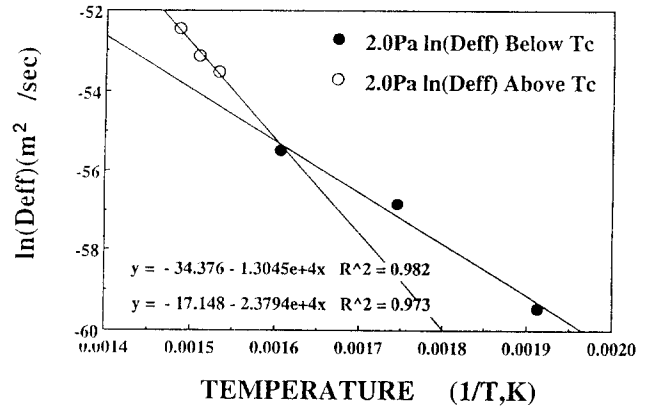
$$E_x = -8.846 \times 10^{-21} \text{ Joule/atom}$$

The negative sign in E_x means that when the angle between the magnetic moments is reduced, the exchange energy is minimized.

To compare the calculated E_x in the above modeling with the difference in activation energy between below and above T_C in experimental interdiffusion results(15), the logarithm of the effective interdiffusion coefficients { $\ln(D_{eff})$ } of the Co/Pd multilayers deposited at 0.7 Pa and 2.0 Pa, respectively, is shown on Fig. 12 (a) and (b) with respect to the reciprocal heat treatment temperature ($1/T$). On both of the figures, 3 points heat treated above T_C lie on linear slope, but the other 3 points heat treated below T_C lie on another linear line. Activation energy (Q) for the interdiffusion process of the Co/Pd multilayers is calculated by slope of Arrhenius equation as follows and listed on Table 2,



(a)



(b)

Fig. 12 (a) and (b): Logarithm of effective interdiffusion coefficients (D_{eff}) of the Co/Pd multilayers deposited at 0.7 Pa and 2.0 Pa, respectively as a function of reciprocal heat treatment temperature

$$D_{eff} = D_0 \exp(-Q/RT) \quad (6)$$

D_{eff} : Effective interdiffusion coefficient (m^2/sec)

D_0 : Pre exponential factor

Q: Activation energy (Joule/Atom)

R: Ideal gas constant(= 8.3170 Joule/Mole)

Comparing with previous researches in D_{eff} which found activation energies of 115 kJ/mole in Mo/Ge[41], 105 kJ/mole in Mo/Si[41], 103 kJ/mole in Pb/Mg[42], 141 kJ/mole in Cu/Au[43] and 106 kJ/mole in Cu/Ni[44] multilayers, the activation energy of the Co/Pd multilayers heat treated above T_C are comparable to these values as shown on Table 2. However, the activation energy heat treated below T_C are almost as twice as that heat treated above T_C . Comparing the difference in Q between below and above T_C , the measured former shows good coincidence with the calculated latter by one order.

Table 2: Activation energy of the Co/Pd multilayers deposited at 0.7 Pa and 2.0 Pa, and heat treated below and above Curie temperature

Co/Pd multilayers	(kJ/mole = 0.01 eV/atom)		
	Activation energy (below T_C)	Activation energy (above T_C)	Difference Between Below and Above T_C
Deposition at 0.7 Pa	253 kJ/mole	128 kJ/mole	125kJ/mole (208 x 10^{-21} J/atom) 92 kJ/mole
Deposition at 2.0 Pa	200 kJ/mole	108 kJ/mole	(153 x 10^{-21} J/atom)

The difference in energy between the modeling and the experiment can be accounted for increased E_x due to the effects of beyond the 1st nearest neighbor pairs and of the expanded polarization of Pd atoms near to the interfaces of the multilayer, which were excluded in the assumptions.

4. Conclusions

The changes in structural stability, i. e. the modulation amplitude and the particle size, of the Co/Pd multilayers as a function of Ar sputtering pressure and heat treatment temperature were investigated with respect to heat treatment time. The sputtering pressure and the heat-treated temperature for the multilayers was divided into 0.7 Pa and 2.0 Pa, and below and above T_c , respectively. The Co/Pd multilayer structure was sequentially changed into 3 parts, which were stress release, interdiffusion and particle growth with respect to the heat treatment time. Little difference in the structural stability of the multilayers deposited at between 0.7 Pa and 2.0 Pa was shown during the above 3 parts. However, the difference heat treated between below and above T_c was shown dramatically. The structural changes below T_c were quite stable, compared with those above T_c in the Co/Pd multilayer. We attribute the stable structural changes to the effect of magnetic exchange energy between magnetic Co sublayers and induced magnetic Pd sublayers when heat-treated below T_c , and recommend the operating temperature range of the Co/Pd multilayer for MO recording just below T_c as the basic research and application, respectively.

References

- [1] P. F. Carcia, A. Suna, D. G. Onn and R. van Antwerp, Superlattices and Microstructures **1**, 101 (1985)
- [2] P. K. Carcia, A. D. meinhardt and A. Suna, J. Appl. Phys. Lett. **47**, 178 (1985)
- [3] F. J. A. denBroeder, H. C. Donkersloot, H. J. G. Draaisma and W. J. M. deJonge, J. Appl. Phys. **61**, 4317 (1985)
- [4] F. J. G. Draaisma, W. J. M. deJonge and F. J. A. denBroeder, J. Magn. Mater. **66**, 351 (1987)
- [5] S. Hashimoto, Y. Ochiai and K. Aso, Jpn J. Appl. Phys. **28**, 1596 (1989)
- [6] M. Hillert, Sc. Ph.D. thesis, Massachusetts Institute of Technology, Cambridge, Massachusetts (1956)
- [7] J. W. Cahn and J. E. Hilliard, J. chem. **28**, 28 (1958)
- [8] Sony technical manual on magneto-optical disc (1992)
- [9] S. Hashimoto, Y. Ochiai and K. Aso, J. Appl. Phys. **67**, 1562 (1993)
- [10] H. Yamane, Y. Maeno and M. Kobayashi, J. Appl. Phys. Lett. **62**, 1562 (1993)
- [11] R. J. Highmore, W. C. Shin, R. E. Somekh and J. E. Evetts, J. Vac. Sci. Technol. A **9**, 2123 (1991)
- [12] B. M. Clements, J. Appl. Phys. **61**, 4525 (1987)
- [13] R. E. Somekh, R. J. Highmore, K. Page, R. J. Home and Z. H. Barber, Mater. Res. Soc. Symp. Proc. **103**, 29 (1988)
- [14] S. Hashimoto, Y. Ochiai and K. Aso, J. Appl. Phys. **66**, 4909 (1989)
- [15] Jai-Young Kim and J. E. Evetts, Journal of Magnetism, Vol. 2 No. 3, 86 (1997)
- [16] R. E. Somekh, R. J. Highmore, K. Page, R. J. Home and Z. H. Barber, Mater. Res. Soc. Symp. Proc. **103**, (1988) 29
- [17] R. E. Somekh and Z. H. Barber, J. Phys. E **21**, 1029 (1988)
- [18] Y. Ochiai, S. Hasimoto and K. Aso, IEEE Trans. MAG **25**, 3755 (1989)
- [19] B. D. Mcwhan, Chapter 2, Synthetic Modulated Structure Ed. by L. L. Chang and B. G. Giessen, Academic press (1985)
- [20] E. Spiller and A. E. Rosenbluth, Proc. SPIE **563**, 221 (1985)
- [21] P. S. Heavens, Optical Properties of Thin Films, (Dover, New York 1965)
- [22] M. U. Hasan, R. J. Highmore and R. E. Somekh, Vacuum **43**, 55 (1992)
- [23] Natl. Bur. Stds. Mono. 25, Sec. **4**, 10 (1965)
- [24] Taylor and Floyd, Acta Cryst. **3**, 285 (1950)
- [25] Swanson and Tatge, Natl. Bur. Stds. Circular **539**, 21 (1953)
- [26] S. Hashimoto, Ph.D. thesis, Nagoya Univ., Nagoya, Japan 15 (1991)
- [27] Y. Suzuki, Researches of the Electrochemical Laboratory, No. **921**, 31 (1991)
- [28] B. D. Engel, C. D. England, R. A. Van Leeuwen, M. H. Wiedmann and C. M. Falco, J. Appl. Phys. MMM-Intermag. **91**, Proceeding, J. Appl. Phys, In Press
- [29] S. T. Durcell, H. W. van Kesteren, E. C. Cosman and W. Hoving, J. Mag. Magn. Mater. **93**, 25 (1991)
- [30] J. Mattson, R. Bhadra, J. B. Ketterson, M. Brodsky and M. Grimsditch, J. Appl. Phys. **67**, 2873 (1990)
- [31] A. L. Greer and F. Spaepen, Chapter 11, Synthetic Modulated Structure Ed. by L. L. Chang and B. G. Giessen, Academic press (1985) 479
- [32] Binary alloy phase diagrams, Vol. 2, 2nd Edition, Ed. by T. B. Massalski, ASM International (1990)
- [33] B. D. Cullity, Elements of X-ray Diffraction 2nd ed. (Addison-Wesley, 1987) 109
- [34] S. Hashimoto, H. Matsuda and Y. Ochiai, Proceedings of SPIE **1248** (1990)
- [35] H. Nakajima and H. Fujimori, The 1846th report of Institute for Materials Research, Tohoku University, Japan (1990) 1

- [36] R. J. Borg and C. E. Birchenall, *Trans. Met. Soc. AIME* **218**, 980 (1960)
- [37] F. S. Buffington, K. Hirano and M. Cohen, *Acta Met.* **9**, 434 (1961)
- [38] G. Hettich, H. Mehrer and K. Maier, *Scripta Metallurgica* **11**, 795 (1977)
- [39] H. Mehrer, D. Hopfel and G. Hettich, *DIMETA-82*, 360 (1983)
- [40] B. D. Cullity, "Introduction to Magnetic Materials", Addison-Wesley, New York (1972) pp. 233
- [41] E. M. Philofsky and J. E. Hilliard, *J. Appl. Phys.* **40**, 2198 (1969)
- [42] W. B. Pearson, *Crystal chemistry and physics of metals and alloys*, Wiley (1972)
- [43] J. Dinklage and R. Frerichs, *J. Appl. Phys* **34**, 2633 (1963)
- [44] W. M. Paulson and J. E. Hilliard, *J. Appl. Phys.* **48**, 2117 (1977)